J. Mol. Biol. (1998) **279**, 271–286

JMB

Conformational Stability and Thermodynamics of Folding of Ribonucleases Sa, Sa2 and Sa3

C. Nick Pace[1,2,3]*, Eric J. Hebert[2], Kevin L. Shaw[2], David Schell[1] Valentin Both[4], Daniela Krajcikova[4], Jozef Sevcik[4], Keith S. Wilson[5] Zbigniew Dauter[5], Robert W. Hartley[6] and Gerald R. Grimsley[1]

[1]*Department of Medical Biochemistry and Genetics and* [2]*Department of Biochemistry and Biophysics and* [3]*Center for Macromolecular Design, Texas A&M University, College Station, TX 77843, USA*

[4]*Institute of Molecular Biology of the Slovak Academy of Sciences, Dubravska cesta 21 842 51 Bratislava, Slovak Republic*

[5]*Department of Chemistry University of York, Heslington York, YO1 5DD, UK*

[6]*Laboratory of Cellular and Developmental Biology, National Institutes of Health Bethesda, MD 20892, USA*

**Corresponding author*

Ribonucleases Sa, Sa2, and Sa3 are three small, extracellular enzymes produced by different strains of *Streptomyces aureofaciens* with amino acid sequences that are 50% identical. We have studied the unfolding of these enzymes by heat and urea to determine the conformational stability and its dependence on temperature, pH, NaCl, and the disulfide bond. All three of the Sa ribonucleases unfold reversibly by a two-state mechanism with melting temperatures, T_m , at pH 7 of 48.4°C (Sa), 41.1°C (Sa2), and 47.2°C (Sa3). The T_m values are increased in the presence of 0.5 M NaCl by 4.0 deg. C (Sa), 0.1 deg. C (Sa2), and 7.2 deg. C (Sa3). The T_m values are decreased by 20.0 deg. C (Sa), 31.5 deg. C (Sa2), and 27.0 deg. C (Sa3) when the single disulfide bond in the molecules is reduced. We compare these results with similar studies on two other members of the microbial ribonuclease family, RNase T_1 and RNase Ba (barnase), and with a member of the mammalian ribonuclease family, RNase A. At pH 7 and 25°C, the conformational stabilities of the ribonucleases are (kcal/mol): 2.9 (Sa2), 5.6 (Sa3), 6.1 (Sa), 6.6 (T_1), 8.7 (Ba), and 9.2 (A). Our analysis of the stabilizing forces suggests that the hydrophobic effect contributes from 90 to 110 kcal/mol and that hydrogen bonding contributes from 70 to 105 kcal/mol to the stability of these ribonucleases. Thus, we think that the hydrophobic effect and hydrogen bonding make large but comparable contributions to the conformational stability of these proteins.

Keywords: ribonucleases; protein folding; protein stability; thermal denaturation; disulfide bonds

Introduction

Ribonucleases (RNases) may be the oldest enzymes, so perhaps it is not surprising that they are involved in such a wide range of functions (Schein, 1997; D'Alessio & Riordan, 1997). The two best characterized families are the mammalian RNases and the microbial RNases. The mammalian RNases, of which RNase A is the best known member, are the most rapidly evolving protein family (Rosenberg *et al*., 1995), and include such RNases as angiogenin, which stimulates blood vessel development, and onconase which is now in clinical trials for cancer treatment (Schein, 1997). The first member of the microbial RNase family to be identified was RNase T_1 (Sato & Egami, 1957). This eukaryotic RNase was found in the culture medium of the fungus *Aspergillus oryzae*, which has been used in making sake since at least the eighth century and in the production of soy sauce (Takamine, 1914). The folding of RNase T_1 has been studied in detail (De Vos *et al*., 1998; Myers *et al*., 1997; Steyaert, 1997; Mayr *et al*., 1996; Pace *et al*., 1991). RNase Ba, from *Bacillus amyloliquefaciens* strain H, was the first prokaryotic RNase to be identified and purified (Nishimura & Nomura, 1959), and its potential usefulness as a protein folding model was shown by Hartley (1968). (RNase Ba is more often known as barnase, but for convenience and consistency with the nomenclature of the other RNases we will use RNase Ba in this paper.) Subsequently, the folding of RNase Ba has been studied in depth by the Fersht laboratory (see Johnson *et al*. (1997) for a recent reference). To

Abbreviations used: DSC, differential scanning calorimitry; ASA, accessible surface area.

0022–2836/98/210271–16 $25.00/0/mb981760

date, over 40 microbial RNases have been identified (Hartley, 1997). Members of the mammalian and microbial RNase families share a small size and a similar mechanism of action.

The *Streptomyces* are Gram-positive filamentous bacteria that are used industrially for the production of several antibiotics. Strains of *Streptomyces aureofaciens* are used to produce the antibiotic chlortetracycline, and they also synthesize and secrete into the growth medium a small RNase (Bacova *et al.*, 1971). The RNases from three of these strains have been characterized and named RNase Sa from strain BMK, RNase Sa2 from strain R8/26, and RNase Sa3 from strain CCM 3239 (Hartley *et al.*, 1996; Hebert *et al.*, 1997). These Sa RNases are members of the microbial ribonuclease family (Hartley, 1980; Hill *et al.*, 1983).

We have expressed RNases Sa, Sa2, and Sa3 in *Escherichia coli* and developed purification procedures that yield from 10 to 50 mg of protein per liter of culture medium (Hebert *et al.*, 1997). RNase Sa is the best characterized of the three enzymes. Crystal structures of native RNase Sa have been determined at 1.8 Å resolution (Sevcik *et al.*, 1991), at 1.2 Å resolution (Sevcik *et al.*, 1996), and most recently at 1.0 Å resolution (Sevcik *et al.*, unpublished observations). In addition, a number of crystal structures have been determined with nucleotides bound (Sevcik *et al.*, 1990, 1993a,b). A solution structure is currently being determined by NMR (M. Rico *et al.*, unpublished observations). Thus, the folded conformation of RNase Sa is extremely well characterized. We have recently completed crystal structures of RNases Sa2 and Sa3 at 1.7 Å resolution (Sevcik *et al.*, unpublished observations).

A ribbon diagram of RNase Sa is shown in Figure 1. The structures of RNases Sa2 and Sa3 are very similar to that of RNase Sa, which is not surprising since the three proteins have identical amino acids at 48 of 96 residues (Figure 2). RNase Sa is the smallest microbial RNase with 96 residues and it is in the $\alpha + \beta$ family of proteins with a three-turn α-helix packed against a five-stranded antiparallel β-sheet to form the hydrophobic core. The Sa RNases contain a single disulfide bond linking Cys residues near the ends of the molecules, e.g. residues 7 and 96 in RNase Sa. When the disulfide bond is broken, the proteins still fold, but the T_m values are lowered from near 50°C to near 20°C (see below). Consequently, at 37°C either the folded protein (disulfide intact) or the unfolded protein (disulfide broken) can be studied, and this is a useful feature. Thus, these RNases can serve as excellent models for both the folded and unfolded states of proteins.

The amino acid sequences of RNases Sa, Sa2, Sa3, Ba, and T_1 are aligned in Figure 2 with the conserved active site residues printed in boldface. All five of these enzymes cleave single-stranded RNA molecules specifically on the 3′ side of guanosine nucleotides. Compared to the 96 residues of RNase Sa , the percent identities are 69% for Sa3, 56% for Sa2, 23% for Ba, and 11% for T_1. RNases Sa, Ba, and T_1 have remarkably similar tertiary structures in the β-sheet regions near the active sites, but there are substantial differences in the α-helices and turns as shown in Figure 1.

Here we report studies of the conformational stability and thermodynamics of folding of RNases Sa, Sa2, and Sa3. We compare these results with similar studies on RNases Ba and T_1, and with studies of mammalian RNase A, a structurally unrelated enzyme with a similar function. Thus, we show how the changes in amino acid sequence have effected the thermodynamics of folding of closely and distantly related relatives in the microbial RNase family. We also compare the con-

Figure 1. Ribbon diagrams of RNases Sa, T_1, and Ba drawn using MOLSCRIPT (Kraulis, 1991) and the following Protein Data Bank entries: 1RGG for RNase Sa, 9RNT for RNase T_1, and 1RNB for RNase Ba.

```
                                                      .                   .
Sa                                            D V S G T V C L S A L P P E A T D T L N L I  22
Sa2                                       A D P A L A D V C R T K L P S Q A Q D T L A L I  24
Sa3                                     A S V K A V G R V C Y S A L P S Q A H D T L D L I  25
Ba  A Q V I N T F D G V A D Y L Q T Y H K L P N D Y I T K S E A Q A L G W V A S K G N L A  43
T1                                  A C D Y T C G S N C Y S S - S D V S T - - A Q A A G Y Q L H  27

                  .                 .                   .
Sa  A S D G P F P Y S Q D G V V F Q N R E S V L P T Q S Y G Y Y H E Y T V - - - - - - - I T  59
Sa2 A K N G P Y P Y N R D G V V F E N R E S R L P K K G N G Y Y H E F T V - - - - - - - V T  61
Sa3 D E G G P F P Y S Q D G V V F Q N R E G L L P A H S T G Y Y H E Y T V - - - - - - - I T  62
Ba  D V A - P G - K S I G G D I F S N R E G K L P G K S G R T W R E A D I - - - - - - N Y T  79
T1  E D G E T V G S N S Y P H K Y N N Y E G F D F S V S S P - Y Y E W P I L S S G D V Y S  69

    .                   .                   .                       .
Sa  P G A R T R G T R R I I T G E A T Q E D Y Y T G D H Y A - - - - T F S L I D Q T C      96
Sa2 P G S N E R G T R R V V T G - G Y G E Q Y W S P D H Y A - - - - T F Q E I D P R C      97
Sa3 P G S P T R G A R R I I T G Q Q W Q E D Y Y T A D H Y A - - - - S F R R V D F A C      99
Ba  S G F - - R N S D R I L Y S S D W - L I Y K T T D H Y Q - - - - T F T K I R           110
T1  G G S P - - G A D R V V F N E N N - Q L A G V I T H T G A S G N N F V E C T           104
```

Figure 2. Aligned amino acid sequences of RNases Sa, Sa2, Sa3, T_1, and Ba (Hebert *et al.*, 1997; Hill *et al.*, 1983).

tributions of conformational entropy, the hydrophobic effect, hydrogen bonding, and disulfide bonds to the conformational stability of these proteins.

Results

Thermal denaturation

Thermal denaturation was studied using both differential scanning calorimetry (DSC) and thermal denaturation curves. Six DSC scans were run on RNase Sa between pH 5.0 and pH 7.0. These experiments were analyzed as described below to determine the midpoint of the thermal denaturation curve, T_m , the calorimetric enthalpy change, ΔH_{cal} , and the van't Hoff enthalpy change, ΔH_{vH}. For the six DSC experiments, the ratio $\Delta H_{cal}/\Delta H_{vH} = 0.99(\pm 0.08)$. For RNases Sa2 and Sa3, two DSC experiments at pH 7 showed that $\Delta H_{cal}/\Delta H_{vH} = 1.00(\pm 0.03)$ (Sa2) and $0.96(\pm 0.04)$ (Sa3). The results from the DSC experiments are in excellent agreement with the results from thermal denaturation curves analyzed assuming a two-state folding mechanism. Thus, the thermal denaturation of all three of the Sa RNases closely approaches a two-state folding mechanism. When DSC scans were repeated on the same sample, almost identical results were obtained, showing that the thermal denaturation of the Sa RNases is reversible. Irreversibility was observed in the DSC experiments at higher protein concentrations near the isoelectric pH (pI) values for the proteins: 3.5 (Sa), 5.3 (Sa2), and 7.2 (Sa3) (Hebert *et al.*, 1997). This appears to result because the unfolded states are also less soluble near their pI values. This is also true of RNase T_1 (Hu *et al.*, 1992).

The circular dichroism (CD) spectra of folded and unfolded RNase Sa are shown in Figure 3(a). The positive CD band near 235 nm is also observed with RNase T_1 and a few other proteins and has been discussed by Woody (1994). This band is not observed in unfolded RNase Sa and the difference between the folded and unfolded CD spectra is greatest at 234 nm, so this was the wavelength chosen to monitor unfolding. A typical thermal denaturation curve is shown in Figure 3(b). Thermal denaturation curves for RNases Sa2 and Sa3 were also determined by measuring the CD at 234 nm, and they are similar to that shown for

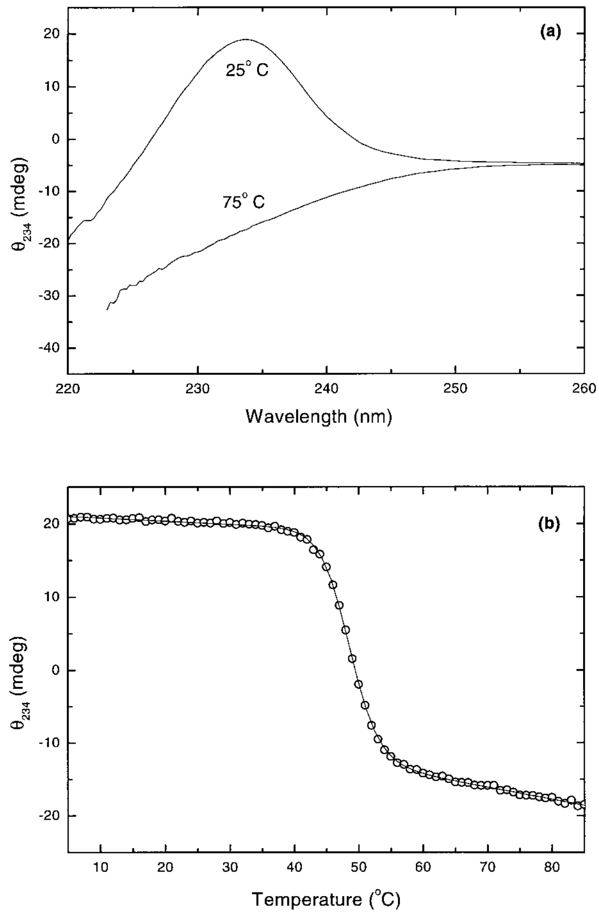

Figure 3. (a) Circular dichroism spectra of native (25°C) and denatured (75°C) RNase Sa in 30 mM Mops buffer (pH 7). (b) A typical thermal denaturation curve for RNase Sa in 30 mM Mops buffer (pH 7) monitored by measuring the circular dichroism at 234 nm. The continuous line is a theoretical curve based on equation (7) and the thermodynamic parameters given in Table 1.

RNase Sa. For all three proteins, thermal denaturation curves were determined as a function of pH over the pH range from 2 to 10. Thermal denaturation was greater than 95% reversible over most of the pH range, and the curves were analyzed by assuming a two-state mechanism. The analyses yield T_m and the van't Hoff enthalpy change for denaturation at T_m, ΔH_m. The thermal denaturation was studied most carefully at pH 7, and these results are summarized in Table 1. At the other pH values, generally only a single thermal denaturation curve was determined and analyzed. These data were used to estimate the heat capacity change for folding, ΔC_p, using the Kirchoff equation:

$$d(\Delta H_m)/d(T_m) = \Delta C_p \quad (1)$$

The plots used to determine ΔC_p values for each of the proteins are shown in Figure 4, and the values are given in Table 1. This method will be discussed further below. Also included in Table 1 are thermodynamic parameters characterizing the folding of RNases Ba, T_1, and A.

Urea denaturation

A typical urea denaturation curve for RNase Sa is shown in Figure 5(a). The urea denaturation curves for RNases Sa2 and Sa3 were similar in appearance and quality. The curves were analyzed by assuming a two-state mechanism, and the fraction of denatured protein, F_D, is plotted as a function of urea concentration for all three proteins in Figure 5(b). From the data in the transition region, the free energy of folding, ΔG, was calculated and found to vary linearly with urea concentration. Consequently, the data were analyzed using the linear extrapolation model:

$$\Delta G = \Delta G(H_2O) - m[\text{urea}] \quad (2)$$

where m is a measure of the dependence of ΔG on urea concentration, and $\Delta G(H_2O)$ is an estimate of the conformational stability of the protein that assumes that the linear dependence of ΔG on urea concentration observed in the transition region continues to 0 M urea (Greene & Pace, 1974; Pace, 1986). The parameters characterizing the urea denaturation of RNases Sa, Sa2, and Sa3 from this study, and of RNases Ba, T_1, and A from the literature are given in Table 2.

Dependence of the conformational stability on NaCl

RNase T_1 is stabilized by NaCl to a much greater extent than RNase A at pH 7 (von Hippel & Wong, 1965; Pace & Grimsley, 1988). The stabilization of RNase T_1 is thought to result from the specific binding of Na ions to the folded protein (Pace & Grimsley, 1988). This prompted us to measure the effect of NaCl on the stability of other members of the microbial RNase family. The results in Table 3 show that all five of the RNases are stabilized by 0.5 M NaCl, but that the increases in T_m range from 0.1 to 7.8°C.

Contribution of disulfide bonds to the conformational stability

The two disulfide bonds in RNase T_1 contribute over 7 kcal/mol to the conformational stability (Pace *et al*., 1988), and the four disulfide bonds in RNase A make such a large contribution to the stability that the protein cannot be folded when the disulfide bonds are broken (Anfinsen, 1973). To assess the contribution of the single disulfide bonds in RNases Sa, Sa2, and Sa3 to their conformational stability, T_m was measured for the proteins in the presence and absence of their disulfide

Table 1. Parameters characterizing the thermal denaturation of selected RNases at pH 7.0

RNase	T_m[a] (°C)	ΔH_m[b] (kcal/mol)	ΔS_m[c] (cal K^{-1} mol^{-1})	ΔC_p[d] (kcal K^{-1} mol^{-1})	$\Delta G(25°C)$[e] (kcal/mol)	T_s[f] (°C)	$\Delta G(T_s)$[e] (kcal/mol)
Sa[g]	48.4	97.4	303	1.52	5.8	−10	9.1
Sa2[g]	41.1	68.4	218	1.27	3.0	−8	5.5
Sa3[g]	47.2	93.6	292	1.57	5.3	−7	8.2
T_1[h]	51.6	105.7	325	1.65	6.8	−7	9.8
Ba[i]	53.2	126.6	388	1.79	8.7	−10	12.8
A[j]	62.8	119.4	355	1.90	9.2	+5	10.5
A[k]	62.8	119.4	355	1.31	10.5	−17	14.8

[a] Midpoint of the thermal unfolding curve. For Sa, Sa2, and Sa3, the standard deviation is ±0.3°C.
[b] Enthalpy change at T_m. For Sa, Sa2, and Sa3, the standard deviation is ±5%.
[c] $\Delta S_m = \Delta H_m / T_m$.
[d] Determined by plotting ΔH_m as a function of T_m using equation (1). The standard deviations are ±0.09 for Sa, ±0.06 for Sa2, and ±0.11 for Sa3.
[e] Calculated with equation (3).
[f] Calculated with equation (4).
[g] From this work.
[h] T_m and ΔH_m are the average of values from Shirley *et al*. (1989, 1992), and Yu *et al*. (1994). ΔC_p is from Pace & Laurents (1989).
[i] T_m and ΔH_m are from this work. ΔC_p is the average value from Johnson & Fersht (1995), and Oliveberg *et al*. (1994).
[j] T_m and ΔH_m are from Catanzano *et al*. (1996). ΔC_p is the average of 13 literature values (Brandts & Hunt, 1967; Danforth *et al*., 1967; Salahuddin & Tanford, 1970; Tsong *et al*., 1970; Shiao *et al*., 1971; Freire & Biltonen, 1978; Schwarz & Kirchoff, 1988; Pace & Laurents, 1989; Barone *et al*., 1992; Makhatadze *et al*., 1995; Liu & Sturtevant, 1996; Catanzano *et al*., 1997).
[k] From Catanzano *et al*. (1996).

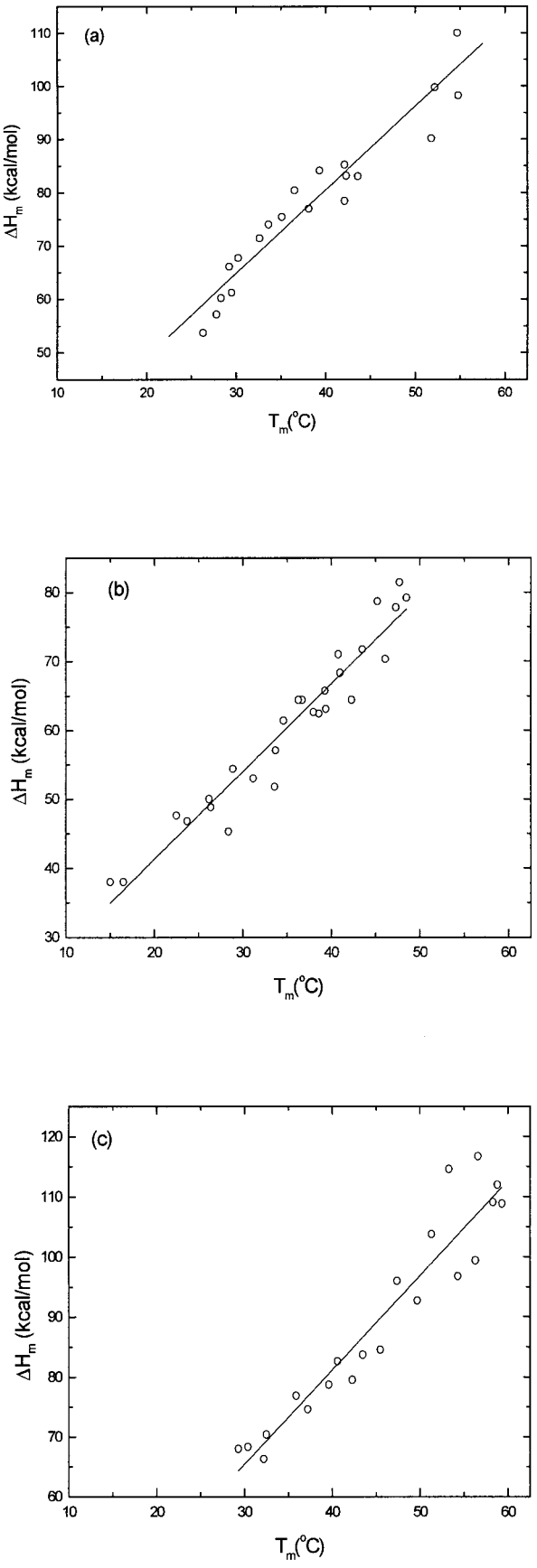

Figure 4. ΔH_m plotted as a function of T_m using data from thermal denaturation curves measured over the pH range 2 to 10 for RNases Sa (a), Sa2 (b), and Sa3 (c). The continuous lines are least-squares fits to equation (1). The values of ΔC_p obtained from this analysis are 1.52(±0.09) for RNase Sa, 1.27(±0.06) for RNase Sa2, and 1.57(±0.11) kcal K^{-1} mol^{-1} for RNase Sa3.

bond. The thermal denaturation curves were determined under different conditions for each protein because their reduced, unfolded states were not soluble at any common pH. (The unfolded states of the proteins are less soluble when the disulfide bonds are reduced.) The results in Table 4 show that the decreases in T_m range from 20°C to 31.5°C, and that the differences in stability at 37°C, a temperature intermediate between the T_m values, range from 5.7 to 7.9 kcal/mol.

Discussion

Thermodynamics of folding

The thermodynamic parameters characterizing the folding of the RNases are given in Table 1. These parameters can be used to calculate the free energy change for folding at any temperature, $\Delta G(T)$, using the modified Gibbs-Helmholtz equation,

$$\Delta G(T) = \Delta H_m(1 - T/T_m) + \Delta C_p[(T - T_m) - T \ln(T/T_m)] \quad (3)$$

and the temperature where $\Delta G(T)$ reaches a maximum, T_S, using

$$T_s = T_m \exp(-\Delta H_m/[T_m \Delta C_p]) \quad (4)$$

(Becktel & Schellman, 1987). The protein stability curves for the six RNases calculated with these equations and the parameters given in Table 1 are shown in Figure 6. Values of T_S, ΔG at T_S, $\Delta G(T_S)$, and ΔG at 25°C, $\Delta G(25°C)$, are given in Table 1. Generally, the value for T_m can be determined to better than ±1%, the value for ΔH_m from a van't Hoff analysis can be determined to about ±5%, and there is good agreement among results from different laboratories. In contrast, there is considerable uncertainty in the ΔC_p values, and different laboratories frequently get conflicting results, even when using the same method. Consider RNase A. A brief search of the literature provided 13 ΔC_p values ranging from 1.24 (Makhatadze *et al.*, 1995) to 2.50 (Brandts & Hunt, 1967) with an average of 1.90(±0.40) kcal K^{-1} mol^{-1}. The last two lines in Table 1 illustrate the importance of ΔC_p in determining T_S , $\Delta G(T_S)$, and $\Delta G(25°C)$. The last line uses a complete data set at pH 7 from Catanzano *et al.* (1996) that includes $\Delta C_p = 1.31$, which is similar to the often-used value from the Privalov lab of 1.29 kcal K^{-1} mol^{-1} (Privalov & Gill, 1988). The next-to-last line uses the average ($C_p = 1.90$ kcal K^{-1} mol^{-1}. Note that the T_S values differ by 22°C, the $\Delta G(T_S)$ values by 4.3 kcal/mol, and the $\Delta G(25°C)$ values by 1.3 kcal/mol, depending just on the value of ΔC_p. This has a dramatic effect on

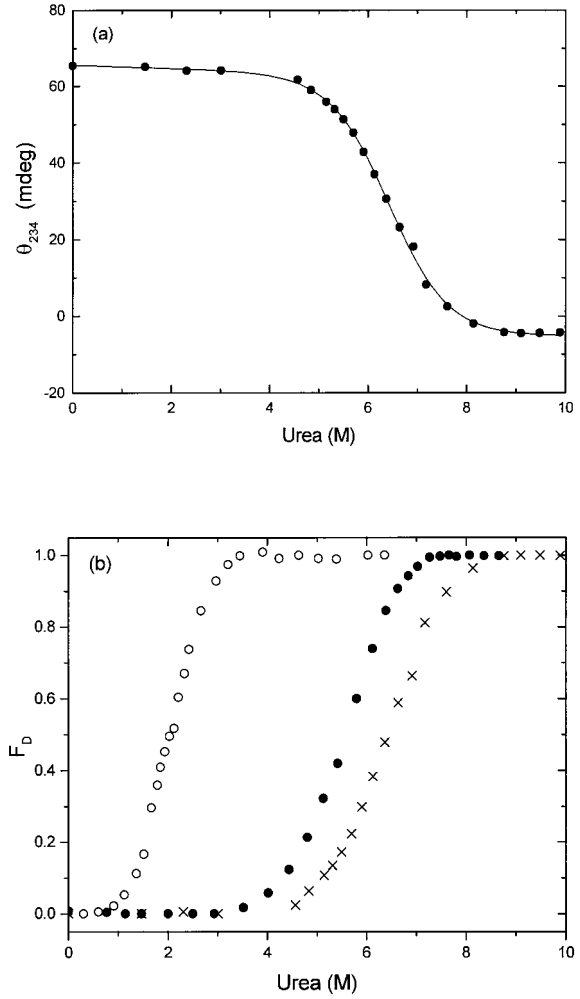

Figure 5. (a) A typical urea denaturation curve for RNase Sa in 30 mM Mops (pH 7.0), 25°C, monitored by measuring the circular dichroism at 234 nm. The continuous line is a theoretical curve based on equation (8) and the parameters given in Table 2. (b) The fraction of denatured protein, F_D, as a function of urea concentration for RNase Sa (×), Sa2 (○), and Sa3 (●) in 30 mM Mops (pH 7.0), 25°C. The points were calculated from data such as those shown in (a) (Pace & Scholtz, 1996).

Table 2. Parameters characterizing the urea denaturation of selected RNases at pH 7.0

RNase	$urea_{1/2}$[a] (M)	m[b] (cal/mol/M)	$\Delta\alpha$[c]	$\Delta G(H_2O)$[b] (kcal/mol)
Sa	6.44	0.99	0.32	6.4
Sa2	2.10	1.31	0.33	2.8
Sa3	5.63	1.05	0.32	5.9
T_1	5.30	1.21	0.32	6.4
Ba	4.49	1.94	0.50	8.7
A	6.92	1.35	0.34	9.3

The data for RNases Sa, Sa2, and Sa3 are from this paper. The data for RNases T_1 and A are from Pace (1990a,b), and the data for RNase Ba are from Pace *et al.* (1992).

[a] $(urea)_{1/2} = \Delta G(H_2O)/m$.

[b] From equation (2)

[c] $\Delta\alpha$ is the fraction of buried groups that must become exposed to solvent on unfolding to account for the measured m values (Pace *et al.*, 1990).

the stability curves, as shown in Figure 6. Consequently, a reliable ΔC_p value is of considerable importance, and below we discuss the methods commonly used to measure ΔC_p.

One DSC method used to determine ΔC_p is to take the difference between the pre- and post-transition baselines. The errors are large because of the uncertainty in the baselines, and the ΔC_p values are generally smaller than those determined by other methods (Schwarz & Kirchoff, 1988). With RNase A, for example, Liu & Sturtevant (1996) found $\Delta C_p = 1.08(\pm 0.14)$ from an analysis of the baselines, and $\Delta C_p = 1.74(\pm 0.02)$ kcal K^{-1} mol^{-1} from a plot of ΔH_{cal} *versus* T_m using equation (1). Thus, the baseline method is not generally used to estimate ΔC_p. However, Privalov *et al.* (1989) have used baseline measurements to show convincingly that ΔC_p decreases with increasing temperature. For example, between 5°C and 50°C they find that ΔC_p decreases from 1.70 to 1.41 for RNase Ba (Griko *et al.*, 1994), and from 1.31 to 1.20 kcal K^{-1} mol^{-1} for RNase T_1 (Yu *et al.*, 1994). This is supported by an analysis of ΔC_p in terms of protein structure and model compound data (Gomez *et al.*, 1995), and, in the case of ubiquitin (Wintrode *et al.*, 1994) and an SH3 domain (Viguera *et al.*, 1994), by the direct observation that ΔH_{cal} does not vary linearly with temperature. In contrast, Nicholson & Scholtz (1996) have shown that a temperature-independent ΔC_p is adequate to describe the stability of histidine-containing phosphocarrier protein over a temperature range from 0°C to 75°C. Our data yield an average ΔC_p for the temperature range 25°C to 55°C, and it is clear that the temperature dependence of ΔC_p can not be determined (Figure 4). Consequently, we assume that ΔC_p is independent of temperature.

The most common DSC method used to determine ΔC_p is to measure ΔH_{cal} as a function of T_m

Table 3. Parameters characterizing the thermal unfolding of five microbial ribonucleases in the presence of 0 M and 0.5 M NaCl

RNase	NaCl (M)	T_m[a] (°C)	ΔT_m[b] (deg. C)	$\Delta(\Delta G)$[c] (kcal/mol)
Sa	0.0	48.4	–	
	0.5	52.4	4.0	1.2
Sa2	0.0	41.1	–	
	0.5	41.2	0.1	0.0
Sa3	0.0	47.2	–	
	0.5	54.4	7.2	2.1
T_1	0.0	51.6	–	
	0.5	59.4	7.8	2.5
Ba	0.0	53.2	–	
	0.5	55.8	2.6	1.0

In 30 mM Mops buffer (pH 7.0).

[a] Midpoint of the thermal unfolding curve.

[b] $\Delta T_m = T_m$ (0.5 M NaCl) $- T_m$ (0 M NaCl).

[c] Determined using the method of Becktel & Shellman (1987), where $\Delta(\Delta G) = \Delta T_m \times \Delta S_m$ using the ΔS_m values from Table 1.

Table 4. Parameters characterizing the contribution of the disulfide bond to the stability of RNases Sa, Sa2, and Sa3

RNase	T_m[a] (°C)	ΔH_m[a] (kcal/mol)	ΔT_m (deg. C)	$\Delta(\Delta G)(T_m)$[b] (kcal/mol)	$\Delta(\Delta G)(37°C)$[b] (kcal/mol)	$\Delta(\Delta G)(25°C)$[b] (kcal/mol)
Sa	48.4	95	–	–	–	–
R-Sa	28.4	87	20	6.8	5.7	4.6
Sa2	48.9	78	–	–	–	–
R-Sa2	17.4	44	31.5	6.8	6.4	5.9
Sa3	50.6	111	–	–	–	–
R-Sa3	23.6	72	27.0	8.4	7.9	7.5

[a] T_m and ΔH_m determined under the following conditions: Sa and R-Sa, 30 mM Pipes buffer (pH 7.0); Sa2 and R-Sa2, 30 mM acetate buffer (pH 5.0); Sa3 and R-Sa3, 30 mM Gly-Gly buffer (pH 3.0).
[b] Determined using equation (3) with the T_m and ΔH_m values from this Table and the ΔC_p values from Table 1.

and use equation (1) (Privalov & Khechinashvili, 1974). The pH is varied to change the stability, and the measurements are generally restricted to the acid pH range of 0 to 5 so that only the carboxyl groups on the protein will ionize. Under these conditions, the heat from proton binding or dissociation will be ≈0 if a carboxyl buffer is used, and no correction to the observed ΔH_{cal} values is necessary. This method has recently been questioned by McCrary *et al*. (1996) on the basis of their studies of the hyperthermophilic protein Sac7d. They find $\Delta C_p = 0.50(\pm 0.02)$ based on plots of ΔH_{cal} *versus* T_m, but $\Delta C_p = 0.86(\pm 0.02)$ kcal K^{-1} mol^{-1} based on a global fit of thermal and chemical denaturation data. They argue convincingly that the higher value is correct, and they show in a subsequent paper that the discrepancy probably results from a failure to take into account the linkage between protein stability and proton and anion binding (McCrary *et al*., 1998). Most proteins bind anions at acid pH and this will probably make a pH dependent contribution to ΔH_{cal} (Fink *et al*., 1994). Anion and cation binding can also contribute directly to ΔC_p. For example, Guinto & Di Cera (1996) have shown that $\Delta C_p = 1.1$ kcal K^{-1} mol^{-1} for the binding of a Na^+ to thrombin. Thus,

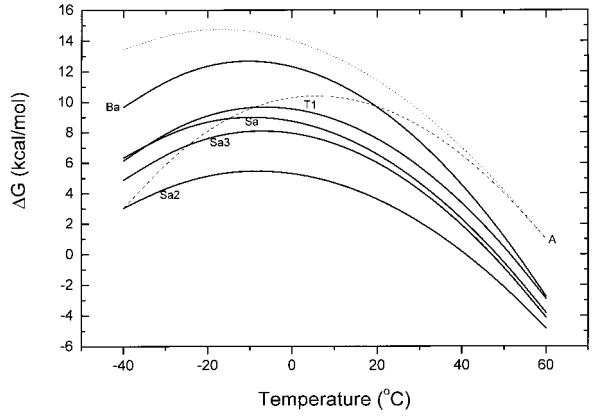

Figure 6. Protein stability curves for RNases Sa, Sa2, Sa3, T_1, Ba, and A at pH 7 calculated using equation (3) and the parameters given in Table 1. For RNase A, the dotted curve is based on $\Delta C_p = 1.31$ and the broken curve is based on $\Delta C_p = 1.90$ kcal K^{-1} mol^{-1} with identical values for ΔH_m and T_m as given in the last two rows in Table 1.

ΔC_p values obtained using ΔH_{cal} values from DSC measurements must be regarded with caution, as emphasized by the studies by Liu & Sturtevant (1996). They found ΔC_p values for RNase A ranging from 1.74 to 3.25 kcal K^{-1} mol^{-1}, depending on the added solute present.

The other approach frequently used to estimate ΔC_p is to measure ΔH_m by a van't Hoff analysis of thermal denaturation curves and again use equation (1). As described above, the measurements are often done in the low pH range, but this is not necessary. This method looks directly at the equilibrium between the folded and unfolded states of the protein. As a consequence, this method yields an effective value of ΔC_p that reflects both protein folding and other effects that shift the protein folding equilibrium. This was the method used to determine the ΔC_p values for RNases Sa, Sa2, and Sa3 given in Table 1. This provides a reliable estimate of ΔC_p over the temperature range 25°C to 50°C and over the pH range 2 to 10. For RNases Ba and T_1, we have chosen the ΔC_p values from the literature that were determined by methods similar to those used here. For RNase A, the average $\Delta C_p = 1.9$ noted above seems more reasonable than the value of 1.24 kcal K^{-1} mol^{-1} that is used in most compilations of ΔC_p values, including ours (Myers *et al*., 1995). This conclusion is based in part on data that indicate that T_S is more likely to be close to 5°C ($\Delta C_p = 1.9$) than to −17°C ($\Delta C_p = 1.31$) (Salahuddin & Tanford, 1970; Arnold & Ulbrich-Hofmann, 1997; G. R. Grimsley, unpublished observations). At present, it seems safest to determine ΔC_p by a global analysis of both thermal and chemical denaturation data (Salahuddin & Tanford, 1967; Pace & Laurents, 1989; Chen & Schellman, 1989; Swint & Robertson, 1993; Scholtz, 1995; Nicholson & Scholtz, 1996; McCrary *et al*., 1996; Grantcharova & Baker, 1997).

Several methods have been proposed to estimate ΔC_p that are based on the changes in accessible surface area that accompany protein folding (Spolar *et al*., 1992; Murphy & Freire, 1992; Myers *et al*., 1995). The best agreement with the ΔC_p values in Table 1 is obtained with:

$$\Delta C_p = -119 + 0.20(\Delta ASA) \qquad (5)$$

where $\Delta(ASA)$ is the change in accessible surface

area exposed on unfolding calculated as described by Myers *et al*. (1995). The values obtained by this equation are (kcal K^{-1} mol^{-1}): 1.36 (Sa), 1.34 (Sa2), 1.39 (Sa3), 1.57 (T_1), 1.79 (Ba), and 1.90 (A), all in reasonable agreement with the experimental values. It might be expected that the four disulfide bonds in RNase A would reduce the value of ΔC_p, but Privalov *et al*. (1989) have shown that ΔC_p does not change significantly when the disulfide bonds are broken.

The results in Table 1 and Figure 6 show that maximum stabilities of the six RNases range from 5.5 to 12.8 kcal/mol. Most other proteins whose conformational stability has been measured would fit in this range (Pace, 1990a). The maximum stabilities occur at similar temperatures, −7°C to −10°C, for the five microbial RNases, but at a somewhat higher temperature for RNase A, 5°C. In addition, the T_m value for RNase A is substantially higher than it is for the microbial RNases. This may reflect the fact that RNase A is adapted to function at 35°C, the temperature of a cow, while the microbial RNases are probably adapted to function at a lower temperature.

Conformational stability at 25°C, pH 7

Estimates of the conformational stability of the RNases at pH 7, 25°C based on analyses of the urea denaturation curves are given in Table 2. It can be seen that these estimates, based on the linear extrapolation method, are in good agreement with the ΔG(25°C) values from thermal denaturation curves given in Table 1. Yao & Bolen (1995) measured stabilities of 9.26(±0.31) and 9.38(±0.12) kcal/mol for RNase A by combining results from urea denaturation and potentiometric titration curves, in remarkably good agreement with stabilities of 9.2 from thermal denaturation (Table 1), 9.3 from urea denaturation (Table 2), and a value of 9.24(±0.64) from GdnHCl denaturation reported previously (Pace *et al*., 1990). Our results suggest that the urea and thermally unfolded states of these proteins are thermodynamically equivalent, and that the linear extrapolation method yields estimates of the conformational stability of the proteins, in good agreement with estimates from thermal denaturation.

There is an excellent correlation between denaturant *m* values (Table 2) and the amount of protein surface area freshly exposed to solvent by unfolding (Myers *et al*., 1995). Tanford (1964, 1970) developed a model that can be used to estimate the fraction of peptide groups and uncharged sidechains that must be exposed to solvent to account for the measured *m* values. We denote this parameter$\Delta\alpha$. We have used this approach to show that proteins unfold to different extents, and that RNase Ba unfolds more completely than RNases T_1 and A (Pace *et al*., 1990, 1992). The $\Delta\alpha$ values in Table 2 show that despite significant differences in the *m* values, the Sa RNases unfold to similar extents and that the extent of unfolding is identical to that observed with RNases T_1 and A. In contrast, RNase Ba unfolds more completely than the other RNases. On the basis of their crystal structures, we estimate that a $\Delta\alpha$ value of ≈0.7 would be observed if a protein unfolded completely. Thus, RNase Ba appears to be about 70% unfolded and the other RNases a little less than 50% unfolded by this criteria. (The analysis uses ΔG_{tr} values from water to denaturant solutions for model compounds so the results actually suggest that the unfolded Sa RNases are only ≈50% as accessible to solvent as the model compounds used to measure the ΔG_{tr} values.) In part, this must reflect the fact that RNase Ba has no disulfide bonds and all of the other RNases do. It also suggests that the single disulfide bonds in the Sa RNases and the two disulfide bonds in RNase T_1 restrict the accessibility to denaturant about the same as the four disulfide bonds in RNase A.

The conformational stability of RNase Sa2 is surprisingly low. With a stability of only 2.9 kcal/mol, one out of 135 molecules is globally unfolded at 25°C. Thus, the low stability would have a small effect on the activity of the enzyme at 25°C and lower temperatures, and evidently this was stable enough for this strain of *Streptomyces* to survive under the conditions that existed as it evolved. The function of these extracellular RNases is not clear so it is difficult to say more about the significance of this exceptionally low stability.

pH dependence of the conformational stability

The T_m and ΔH_m values measured as a function of pH were used with the ΔC_p values from Table 1 to calculate ΔG(25°C) values as a function of pH using equation (3), and the results are shown in Figure 7. Studies of the pH dependence of stability for the other RNases have been published: RNase T_1 (Pace *et al*., 1990; Hu *et al*., 1992; Barone *et al*., 1992; Yu *et al*., 1994), RNase Ba (Pace *et al*., 1992; Oliveberg *et al*., 1994; Griko *et al*., 1994), and RNase A (Pace *et al*., 1990; Barone *et al*., 1992; Yao & Bolen, 1995). At the pH of maximum stability, the stabilities of the proteins are (kcal/mol): 4.7 (Sa2), 7.0 (Sa), 8.6 (Sa3), 8.8 (T_1), 9.0 (Ba), and 9.3 (A). The microbial RNases are all maximally stable near pH 5 and most active in RNA hydrolysis at pH 7.5 to 8, despite a wide range of isoelectric points: 3.5 (Sa), 3.7 (T_1), 5.3 (Sa2), 7.2 (Sa3), and 9.3 (Ba) (Hebert *et al*., 1997; Mossakowska *et al*., 1989). This suggests that it is advantageous for these proteins to maximize their stability near pH 5 and their activity near pH 7.5, but that there is no selective pressure to maintain a particular isoelectric point.

The stability of all of the RNases drops sharply as the pH decreases below pH 4 (Figure 7). This is because some of the carboxyl groups have lower p*K* values in the folded than in the unfolded proteins. In RNase A, for example, five of the 11 car-

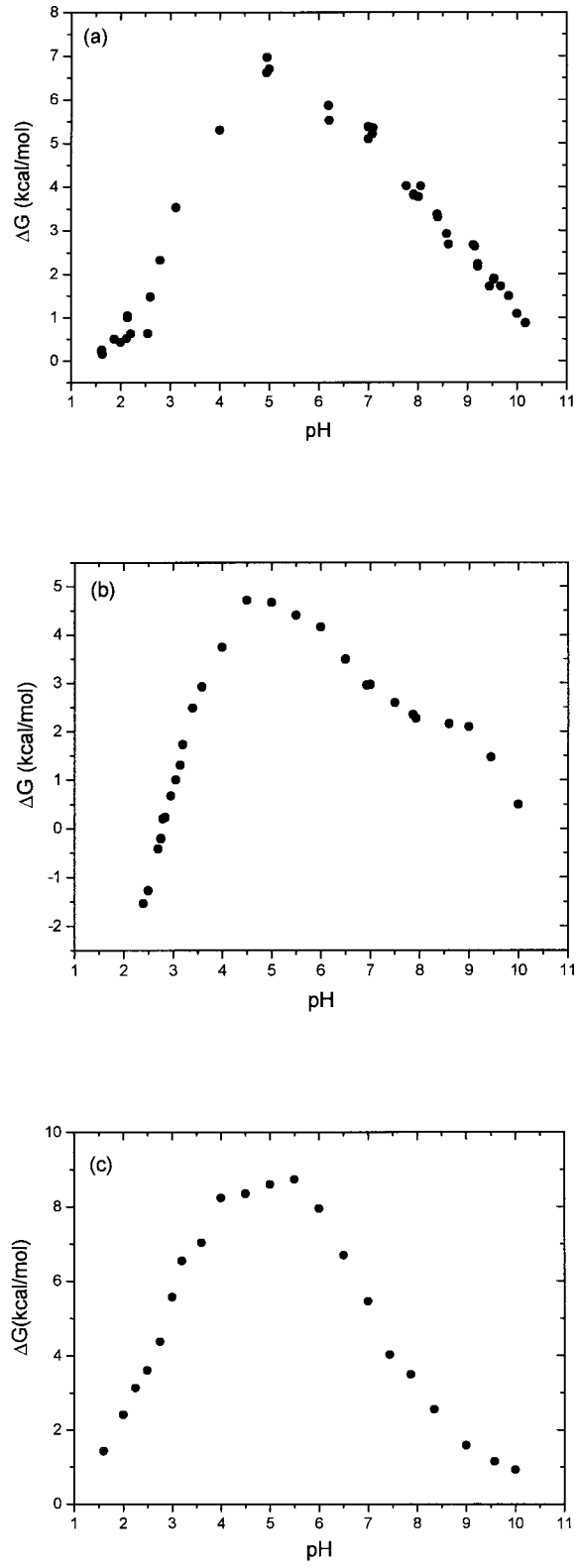

Figure 7. Conformational stability, $\Delta G(25^{\circ}C)$, as a function of pH for RNase Sa (a), RNase Sa2 (b), and RNase Sa3 (c). $\Delta G(25^{\circ}C)$ was calculated using equation (3) with ΔH_m and T_m values from thermal denaturation curves measured over the pH range 2 to 10 (the same data shown in Figure 4), and the ΔC_p values given in Table 1.

boxyl groups have pK values less than 3 in the folded protein and they would all be expected to have values above 4 in the unfolded proteins (Baker & Kintanar, 1996; Rico *et al.*, 1991). As a consequence, the unfolded states bind protons more tightly than the folded states, and the equilibrium will be shifted toward unfolding as the H^+ concentration increases. The dependence of $\Delta G(25^{\circ}C)$ on pH can be used to estimate the maximum number of protons taken up on unfolding. The numbers range from ≈2 for RNases T_1 and A (Pace *et al.*, 1990), to ≈3 for the Sa RNases, to ≈4 for RNase Ba (Oliveberg *et al.*, 1994). At higher pH values, the stabilities of the proteins drop showing that some of the ionizable groups in the folded proteins now have higher pK values than the same groups in the unfolded proteins. Note in Figure 7 that each of the Sa RNases has a unique dependence of stability on pH above pH 5. In both RNase T_1 (McNutt *et al.*, 1990) and RNase Ba (Sali *et al.*, 1988; Pace *et al.*, 1992), the pH dependence between pH 5 and 9 has been shown to depend mainly on a difference in the pK values of histidine side-chains in the folded and unfolded proteins. We are currently attempting to measure the pK values of all of the ionizable side-chains in folded and unfolded RNase Sa to see if they can be used to account quantitatively for the observed pH dependence of the stability.

NaCl dependence of the conformational stability

The conformational stability of a protein is often affected by the type and concentration of salt present. This can result from (1) an ionic strength effect due to Debye-Huckel screening of electrostatic interactions that contribute to protein stability, (2) the effects of salts on the groups which are exposed to solvent when the protein unfolds, and (3) the preferential binding of cations or anions to either the native or denatured states of the protein (von Hippel & Wong, 1965; Schrier & Schrier, 1967). We have shown that the conformational stability of RNase T_1 is increased by salts and can be doubled by adding 0.2 M Na_2HPO_4. This remarkable increase in the conformational stability results primarily from the preferential binding of cations and anions to folded RNase T_1 (Pace & Grimsley, 1988). To see if salts have a similar effect on the conformational stability of the other microbial RNases, we determined thermal unfolding curves at pH 7 in the presence and absence of 0.5 M NaCl. The results in Table 3 show that the presence of 0.5 M NaCl increases the stability of RNases Sa3 and T_1 by over 2 kcal/mol, increases the stability of RNases Sa and Ba by about 1 kcal/mol, but has no effect on the stability of RNase Sa2. As for RNase T_1, it seems likely that most of the stability enhancement of RNases Sa, Sa3, and Ba is due to the preferential binding of cations or anions by the folded conformations of the proteins.

The least stable of the RNases, Sa2, is the only protein that is not stabilized significantly by NaCl.

Contribution of disulfide bonds to the conformational stability

The Sa RNases each contain a single disulfide bond at equivalent positions that links the ends of the molecule, e.g. residues 7 and 96 in RNase Sa (Figure 2). The three disulfide bonds are buried to similar extents, 62, 66, and 60% buried, have similar S to S distances, 2.03, 2.00, and 2.00 Å, and have similar χ_3 angles, -94°, -86°, and -94°, for RNases Sa, Sa2, and Sa3, respectively. However, they affect the stabilities of the proteins to different extents. The ΔT_m values range from 20 deg. C to 31.5 deg. C, but the difference in stability depends on the temperature chosen for the comparison. We have not measured ΔC_p values for the reduced proteins so we have used the ΔC_p values from Table 1 to compare the stabilities at different temperatures. In the case of RNase Ba, Johnson *et al.* (1997) have shown that the presence of additional disulfide bonds does not change the ΔC_p values to a great extent. The results in Table 4 show that the $\Delta(\Delta G)$ values are greatest at the T_m of the proteins with their disulfides intact and decrease at lower temperatures.

Disulfide bonds increase the conformational stability of a protein primarily by constraining the unfolded conformations of the protein and thereby decreasing their conformational entropy. Based on our studies with RNase T_1 and the few other studies available in the literature at the time, we suggested that the following equation could be used to roughly estimate the effect of a cross-link on the conformational entropy:

$$\Delta S = -2.1 - (3/2)R \ln n \qquad (6)$$

where n is the number of residues in the loop forming the cross-link (Pace *et al.*, 1988). For the Sa RNases, this suggests that the disulfide bonds would contribute 4.8 kcal/mol to the stability at 25°C. It can be seen in Table 4 that this provides a good estimate of the contribution of the disulfide bond to the stability of RNase Sa, but that the disulfide bonds of RNases Sa2 and Sa3 make a greater contribution to the stability. This is not surprising since factors such as strain in the native state (Katz & Kossiakoff, 1986), the hydrophobic effect (Doig & Williams, 1991), and other factors (Zhang *et al.*, 1994) can also make important contributions.

Forces contributing to the conformational stability of the microbial RNases

We have used the crystal structures of the RNases to gain insight into the forces that contribute to their conformational stability. The major force favoring the unfolded state is conformational entropy. Rotation around the many bonds in a protein increases dramatically when the protein unfolds, and this provides a strong entropic driving force for unfolding. Substantial progress has been made in estimating the conformational entropy change accompanying protein folding, ΔS_{CE}. Spolar & Record (1994) used an approach that separates the contribution of the hydrophobic effect to ΔS for protein folding from the other contributions, which they argue are mainly conformational entropy. They find $\Delta S_{CE} = 5.6(\pm 0.5)$ kcal K^{-1} mol^{-1} per residue, and this translates into a contribution to ΔG at 25°C of 1.7 kcal/mol per residue. When this is applied to the RNases, the results shown in Table 5 are obtained. In a completely different approach, the Freire lab used a combination of theory and experiment to arrive at a method for estimating the residue-specific changes in side-chain and backbone conformational entropy that accompany protein folding (Lee *et al.*, 1994; D'Aquino *et al.*, 1996). Estimates based on this

Table 5. Forces contributing to the conformational stability of the RNases

RNase	C.E.[a]	C.E.[b]	S-S[c]	HP[d]	HB[e]	ΔG(pred)	ΔG(25°C)
Sa	163	165	5	88	85	13	6
Sa2	165	168	6	92	79	9	3
Sa3	168	167	8	91	69	1	5
T_1	177	187	7	88	96	4	7
Ba	187	196	0	112	92	8	9
A	211	224	15	112	106	9	9

All units are kcal/mol.

[a] Conformational entropy calculated using 1.7 kcal/mol per residue (Spolar & Record, 1994).

[b] Conformational entropy calculated as described by Lee *et al.* (1994) and D'Aquino *et al.* (1996).

[c] Values at 25 °C for RNases Sa, Sa2, and Sa3 are from Table 4; for RNase T_1 are from Pace *et al.* (1988); and for RNase A were calculated using equation (6).

[d] The contribution of the hydrophobic effect, HP, was calculated by multiplying the ΔG_{tr} values for *n*-octanol (Fauchere & Pliska, 1983; Pace, 1995) by the number of hydrophobic groups buried estimated by the Lee & Richards (1971) program. The hydrophobic groups included were the -CH_2- groups from all of the polar and charged residues, plus the side-chains of the following amino acids: Ala, Val, Ile, Leu, Pro, Phe, Tyr, Trp, Met, Cys.

[e] The contribution of hydrogen bonding, HB, was calculated by multiplying the number of hydrogen bonds calculated using the HBPLUS program from McDonald & Thornton (1994) by 1.0 kcal/mol per hydrogen bond (Myers & Pace, 1996).

approach are also given in Table 5, and they are in remarkable agreement with those from the Spolar & Record (1994) approach. We will use the estimates based on the Freire method for the rest of the analysis because they make use of the three-dimensional structures to estimate the extent to which each residue is buried in the folded protein, and we have this information for the RNases.

One means of overcoming ΔS_{CE} is to introduce disulfide bonds which will restrict the conformational entropy of the unfolded protein. In the microbial RNase family, the number of disulfide bonds ranges from zero to three, but most of the members have at least one disulfide bond. As shown in Table 5, the single disulfide bond that crosslinks the ends of the Sa RNases contributes from 5 to 8 kcal/mol to the stability at 25°C, and the two disulfide bonds in RNase T_1 contribute 7 kcal/mol to the stability. The contribution of the disulfide bonds to the conformational stability of RNase A is a rough estimate based on equation (7). The Scheraga lab (Laity *et al*., 1997) is investigating the disulfide bonds of RNase A in detail and have shown experimentally that removing the 40 to 95 disulfide bond in RNase A lowers the T_m value by 22 deg. C. Using equation (3), we find that this corresponds to a decrease in stability of 5.8 kcal/mol at 25°C. Disulfide bonds are most often found in extracellular enzymes, and all of the microbial RNases are extracellular. It might prove interesting to study the evolution of disulfide bonds in the microbial RNases family. It is possible that disulfide bonds provide other advantages to an organism besides their contribution to protein stability.

Since Kauzmann's (1959) classic review, the prevailing view has been that the hydrophobic effect is the major force stabilizing proteins. We have suggested, based on stability studies of hydrophobic mutants (Xu *et al*., 1998), that ΔG_{tr} values for the transfer of hydrophobic groups from water to *n*-octanol can be used to obtain a reasonable estimate of the contribution of the hydrophobic effect to protein stability (Pace *et al*., 1996). We have used the crystal structures of the proteins to estimate the number of hydrophobic side-chains (Ala (3.4/6), Val (4.6/6), Ile (4.3/5), Leu (5.1/6), Pro (2.5/6), Phe (2.7/3), Tyr (6.2/8), Trp (0/0), Met (0/0), Cys (1.3/2)), and the number of -CH_2- groups from the polar and charged side-chains (43.7/79) that are buried on folding. (The values for RNase Sa are given in parentheses (number buried/number present) as an example.) These are then multiplied by the appropriate ΔG_{tr} value based on the *n*-octanol data (Fauchere & Pliska, 1983; Pace, 1995), and the contributions summed to arrive at the estimate of the contribution of the hydrophobic effect to the stability of each RNase given in Table 5. Note that the hydrophobic effect contributes more to the stability of RNases Sa, Sa2, and Sa3 than to RNase T_1, a larger protein. Note also that the hydrophobic effect makes the same contribution to RNase Ba as to RNase A, a protein with 14 more residues. It is clear that the contribution of disulfide bonds and the hydrophobic effect is not sufficient to overcome the unfavorable contribution from conformational entropy. We propose that the additional free energy must come from the burial and hydrogen bonding of the polar groups in protein folding.

When a peptide group is transferred from water to the vapor phase, the dehydration is very unfavorable, $\Delta G_{tr} = 12.1$ kcal/mol (Makhatadze & Privalov, 1995). When a peptide group is transferred from water to cyclohexane, the dehydration is much less unfavorable, $\Delta G_{tr} = 5.3$ kcal/mol (Radzika & Wolfenden, 1988; Pace, 1995). This shows unequivocally that van der Waals interactions between the peptide group and cyclohexane are very favorable. The interior of a protein is considerably more tightly packed than cyclohexane (Harpaz *et al*., 1994) so the van der Waals interactions will be even more favorable when a peptide group is buried in protein folding. Thus, we disagree with Honig & Cohen (1996) when they conclude: "$\cdots$ a crucial property of the polypeptide backbone is that it contains polar NH and CO groups whose removal from water involves a significant energetic penalty." We think that polar group burial in the protein interior is not so costly so that when polar groups are buried and form hydrogen bonds there is a substantial net gain in stability (Myers & Pace, 1996). Studies of 52 hydrogen bonding mutants show that when a hydrogen-bonded polar group is removed from a protein, the average $\Delta(\Delta G) = 1.0(\pm 1.0)$ kcal/mol per hydrogen bond (Myers & Pace, 1996). For each of the RNases, we have estimated the number of hydrogen bonds formed on folding using the HBPLUS program of McDonald & Thornton (1994). The product of these numbers leads to the estimates of the contribution of intramolecular hydrogen bonding to the stability of the RNases given in Table 5. Only for RNase T_1 is the contribution from hydrogen bonding greater than the contribution from the hydrophobic effect, but the values are always comparable in magnitude, with the biggest difference being 22 kcal/mol for RNase Sa3. It is interesting that the contribution of hydrogen bonding to the stability of the three Sa RNases varies over a wider range than the contribution of the hydrophobic effect. The average lengths of the hydrogen bonds in the six proteins are (Å): 2.92 (Sa2), 2.93 (Ba), 2.94 (A), 2.95 (T_1), 2.96 (Sa3), and 2.97 (Sa). It is not clear if these differences are significant, since other factors such as geometry are important, but there are indications that it may be (Makhatadze & Privalov, 1995).

When the three stabilizing contributions and the destabilizing contribution are summed, we arrive at the predicted conformational stabilities, ΔG(pred), given in Table 5 along with the measured values, ΔG(25°C). The agreement is remarkably good given the number of factors that are ignored and this suggests that the major forces contributing to the conformational stability of proteins are included in Table 5.

In conclusion, this analysis of the stability of these RNases provides additional support for the idea that intramolecular hydrogen bonding does indeed provide a favorable contribution to protein stability, and that the contribution is comparable in magnitude to that of the hydrophobic effect.

Materials and Methods

Materials

The purification of RNases Sa, Sa2, and Sa3 after expression into the periplasmic space of *Escherichia coli* is described by Hebert *et al*. (1997). The expression and purification of RNase Ba is described by Okorokov *et al*. (1994). Protein concentrations were determined using molar absorption coefficients at 278 nm of 12,300 M^{-1} cm^{-1} (1.16 mg^{-1} ml cm^{-1}, Sa), 17,100 M^{-1} cm^{-1} (1.57 mg^{-1} ml cm^{-1}, Sa2), 17,550 M^{-1} cm^{-1} (1.59 mg^{-1} ml cm^{-1}, Sa3) (Hebert *et al*., 1997), and 25,880 M^{-1} cm^{-1} (2.09 mg^{-1} ml cm^{-1}, Ba) (Lees & Hartley, 1966). Ultrapure urea was purchased from Ambion. Reagent-grade chemicals and glass-distilled water were used to prepare all buffers and solutions.

R-RNases Sa, Sa2, and Sa3 were prepared using the methods described by Pace & Creighton (1986). In brief, the enzymes were reduced by incubating for two to three hours at 25°C in 0.2 M Tris-HCl (pH 8.7), 2 mM EDTA, 6 M guanidine hydrochloride, and 0.1 M dithiothreitol. This mixture was then desalted with a Sephadex G-25 column equilibrated with 10 mM dithiothreitol in the desired buffer. The reduced protein was used for unfolding studies on the same day of preparation. The dithiothreitol was purchased from Sigma.

Thermal and urea denaturation

Urea and thermal denaturation curves were determined using circular dichroism measurements at 234 nm to follow unfolding. The general approach is described by Pace & Scholtz (1996). The instrument was an Aviv 62DS spectropolarimeter equipped with a temperature control and stirring unit. We typically used protein concentrations of 0.05 to 0.2 mg/ml and quartz cuvettes with a 1 cm path length.

For thermal denaturation curves, measurements were typically made at one degree intervals between 0°C and 80°C, at a heating rate of 30 deg. C/hour (equilibration time between measurements = 1.5 minutes, band width = 10 nm, and time constant = ten seconds). Following the approach of Santoro & Bolen (1988), a non-linear least-squares analysis was used to fit the thermal denaturation curves to the equation:

$$y = \{(y_f + m_f \cdot [T]) + (y_u + m_u \cdot [T]) \cdot \exp[(\Delta H_m/RT) \cdot ((T - T_m)/T_m)]\}/(1 + \exp[(\Delta H_m/RT) \cdot ((T - T_m)/T_m]) \quad (7)$$

where y represents the observed circular dichroism signal at 234 nm, y_f and y_u are the intercepts and m_f and m_u the slopes of the pre- and posttransition baselines, T is the temperature, T_m is the midpoint of the thermal unfolding curve, and ΔH_m is the enthalpy change for unfolding at T_m. Curve-fitting was performed using MicroCal Origin version 2.9 curve fitting software (MicroCal Software, Inc., Northampton, MA). Reversibility of thermal denaturation in the pH range from 2 to 10 was checked by reheating the sample. In this pH range, the reversibility was greater than 95% as judged by comparison of the ΔH_m values for the two scans. The buffers used were: glycine (pH 1.5 to 3.5 and 9.5 to 10), acetate (pH 3.5 to 5.5), Mes (pH 5.5 to 6.5), Mops (6.5 to 8.5), and diglycine (8.5 to 9.5).

Urea stock solutions were prepared and their molarity calculated as described (Pace, 1986). Urea denaturation curves were determined by directly adding increasing amounts of urea to a single protein solution, with a correction made for the increase in reaction volume (Nicholson & Scholtz, 1996). Urea denaturation was shown to be greater than 95% reversible for all of the conditions reported here. A non-linear least-squares analysis was used to fit the urea denaturation curves to the equation (Pace & Scholtz, 1996):

$$y = \{(y_f + m_f \cdot [D]) + (y_u + m_u \cdot [D]) \cdot \exp[m \cdot ([D] - [D]_{1/2})/RT]\}/(1 + \exp[m \cdot ([D] - [D]_{1/2})/RT]) \quad (8)$$

where y represents the observed circular dichroism at 234 nm, y_f and y_u are the intercepts and m_f and m_u are the slopes of the pre- and posttransition baselines, $[D]$ is the urea concentration, $[D]_{1/2}$ is the urea concentration at the midpoint of the curve, and m is from equation (2). The curves were analyzed with the same software used to analyze the thermal denaturation curves.

Differential scanning calorimetry

Differential scanning calorimetry (DSC) was performed on a Microcal MC2 DSC running MC2Plus EMF data acquisition software. Protein samples (5 to 10 ml of a 0.5 to 2.0 mg ml^{-1} solution) were dialyzed twice against two litres of buffer (30 mM) for at least four hours at 4°C. After the second dialysis, the protein sample and ≈50 ml of dialysate were centrifuged at 15,000 rpm for 20 minutes in a Sorvall SS-34 rotor at 4°C and degassed for ten minutes. Dialysate buffer was used in both cells to determine baselines that were subtracted from the sample runs to generate the DSC scans that were analyzed. Dialysate buffer was also used in the reference cell for all DSC sample scans. Data were collected under 40 lb/in^2 of nitrogen using a 45 deg. C/hour scan rate and a 20 second filter constant. A second scan was run on each sample after a 90 minute equilibration at low temperature to check thermal reversibility. The 30 mM buffers used were the sodium salts of Mes (pH 5.0 to 6.5), Mops (pH 6.0 to 7.9), or Pipes (pH 6.0 to 7.9). The DSC data were analyzed using the program *dscII* (E.J. Hebert & K. Gajiwala, Texas A&M University, College Station, TX). The calorimetric enthalpy of unfolding, ΔH_{cal}, was calculated using a composite Simpson's rule and a sigmoidal progression baseline. T_m was the temperature at which half of the total heat had been absorbed (Freire, 1995). The van't Hoff enthalpy, ΔH_{vH}, was obtained using:

$$\Delta H_{vH} = 4R(T_m)^2 \Delta C_{p,max}/\Delta H_{cal} \quad (9)$$

where $C_{p,max}$ is the maximum of the excess heat capacity (Privalov & Khechinashvili, 1974).

Acknowledgments

This research was supported by grants from the National Institutes of Health (GM 37039), the Robert A. Welch Foundation (A 1060), The Texas Advanced

Research Program (010366-181), and by the Tom and Jean McMullin Professorship. We thank Marty Scholtz, Eric Nicholson, Mary Elizabeth Huffine, Bea Huyghues-Despointes, George Makhatadze, and Norm Pace for helpful discussions.

References

Anfinsen, C. B. (1973). Principles that govern the folding of protein chains. *Science,* **181**, 223–230.

Arnold, U. & Ulbrich-Hofmann, R. (1997). Kinetic and thermodynamic stabilities of ribonuclease A and ribonuclease B. *Biochemistry,* **36**, 2166–2172.

Bacova, M., Zelinkova, E. & Zelinka, J. (1971). Exocellular ribonuclease from *Streptomyces aureofaciens*. *Biochim. Biophys. Acta.* **235**, 335–342.

Baker, W. R. & Kintanar, A. (1996). Characterization of the pH titration shifts of ribonuclease A by one- and two-dimensional nuclear magnetic resonance spectroscopy. *Arch. Biochem. Biophys,* **327**, 189–199.

Barone, G., Del, Vecchio P., Fessas, D., Giancola, C., Graziano, G., Pucci, P., Riccio, A. & Ruoppolo, M. (1992). Thermal denaturation of ribonuclease T_1: a DSC study. *J. Therm. Anal.* **38**, 2791–2802.

Becktel, W. J. & Schellman, J. A. (1987). Protein stability curves. *Biopolymers,* **26**, 1859–1877.

Brandts, J. F. & Hunt, L. (1967). The thermodynamics of protein denaturation. III. The denaturation of ribonuclease in water and aqueous urea and aqueous ethanol mixtures. *J. Am. Chem. Soc.* **89**, 4826–4838.

Catanzano, F., Giancola, C., Graziano, G. & Barone, G. (1996). Temperature-induced denaturation of ribonuclease S: a thermodynamic study. *Biochemistry,* **35**, 13378–13385.

Catanzano, F., Graziano, G., Capasso, S. & Barone, G. (1997). Thermodynamic analysis of the effect of selective monodeamidation on asparagine 67 in ribonuclease A. *Protein Sci.* **6**, 1682–1693.

Chen, B. & Schellman, J. A. (1989). Low-temperature unfolding of a mutant of phage T4 lysozyme. 2. Equilibrium studies. *Biochemistry,* **28**, 691–699.

D'Alessio, G. & Riordan, J. F. (1997). *Editors of Ribonucleases,* Academic Press, San Diego.

Danforth, R., Krakauer, H. & Sturtevant, J. M. (1967). Differential calorimetry of thermally induced processes in solution. *Rev. Sci. Instrum.* **38**, 484–487.

D'Aquino, J. A., Gomez, J., Hilser, V., Lee, K. H., Amzel, L. M. & Friere, E. (1996). The magnitude of the backbone conformational entropy change in protein folding. *Proteins: Struct. Funct. Genet.* **25**, 143–156.

De Vos, S., Doumen, V., Langhorst, U. & Steyaert, J. (1998). Dissecting histidine interactions of ribonuclease T_1 with asparagine and glutamine replacements: analysis of double mutant cycles at one position. *J. Mol. Biol.* **275**, 651–661.

Doig, A. J. & Williams, D. H. (1991). Is the hydrophobic effect stabilizing or destabilizing in proteins? The contribution of disulphide bonds to protein stability. *J. Mol. Biol.* **217**, 389–398.

Fauchere, J. L. & Pliska, V. E. (1983). Hydrophobic parameters of amino-acid side chains from the partitioning of *N*-acetyl-amino-acid amides. *Eur. J. Med. Chem.* **18**, 369–375.

Fink, A. L., Calciano, L. J., Goto, Y., Kurotsu, T. & Palleros, D. R. (1994). Classification of acid denaturation of proteins: intermediates and unfolded states. *Biochemistry,* **33**, 12504–12511.

Friere, E. (1995). Differential scanning calorimetry. In *Protein Stability and Folding: Theory and Practice* (Shirley, B. A., ed.), pp. 191–218, Humana Press, Totowa, New Jersey.

Freire, E. & Biltonen, R. (1978). Statistical mechanical deconvolution of thermal transitions in macromolecules. I. Theory and application to homogeneous systems. *Biopolymers,* **17**, 463–479.

Gomez, J., Hilser, V. J., Xie, D. & Friere, E. (1995). The heat capacity of proteins. *Proteins: Struct. Funct. Genet.* **22**, 404–412.

Grantcharova, V. P. & Baker, D. (1997). Folding dynamics of the src SH3 domain. *Biochemistry,* **36**, 15685–15692.

Greene, R. F. & Pace, C. N. (1974). Urea and guanidine hydrochloride denaturation of ribonuclease, lysozyme, α-chymotrypsin, and β-lactoglobulin. *J. Biol. Chem.* **249**, 5388–5393.

Griko, Y. V., Makhatadze, G. I., Privalov, P. L. & Hartley, R. W. (1994). Thermodynamics of barnase unfolding. *Protein Sci.* **3**, 669–676.

Guinto, E. R. & Di Cera, E. (1996). Large heat capacity change in a protein-monovalent cation interaction. *Biochemistry,* **35**, 8800–8804.

Harpaz, Y., Gerstein, M. & Chothia, C. (1994). Volume changes in protein folding. *Structure,* **2**, 641–649.

Hartley, R. W. (1968). A reversible thermal transition of the extracellular ribonuclease of *Bacillus amyloliquefaciens*. *Biochemistry,* **6**, 2401–2408.

Hartley, R. W. (1980). Homology between prokaryotic and eukaryotic ribonucleases. *J. Mol. Evol.* **15**, 355–358.

Hartley, R. W. (1997). Barnase and barstar. In *Ribonucleases* (D'Alessio, G. & Riordan, J., eds), pp. 51–100, Academic Press, San Diego.

Hartley, R. W., Both, V., Hebert, E. J., Homerova, D., Jucovic, M., Nazarov, V., Rybajlak, I. & Sevcik, J. (1996). Barstar inhibits extracellular ribonucleases of *Streptomyces* and allows their production from recombinant genes. *Protein Pept. Letters,* **3**, 225–231.

Hebert, E. J., Grimsley, G. R., Hartley, R. W., Horn, G., Schell, D., Garcia S., , Both, V., Sevcik, J. & Pace, C. N. (1997). Purification of ribonucleases Sa, Sa2, and Sa3 after expression in *Escherichia coli*. *Protein Express. Purificat.* **11**, 162–168.

Hill, C., Dodson, G., Heinemann, U., Saenger, W., Mitsui, Y., Nakamura, K., Borisov, S., Tischenko, G., Polyakov, K. & Pavlovsky, S. (1983). The structural and sequencehomology of a family of microbial ribonucleases. *Trends Biochem. Sci.* **8**, 364–369.

Honig, B. & Cohen, F. E. (1996). Adding backbone to protein folding: why proteins are polypeptides. *Folding Design,* **1**, R17–R20.

Hu, C., Sturtevant, J. M., Thomson, J. A., Erickson, R. E. & Pace, C. N. (1992). Thermodynamics of ribonuclease T_1 denaturation. *Biochemistry,* **31**, 4876–4882.

Johnson, C. M. & Fersht, A. R. (1995). Protein stability as a function of denaturant concentration: the thermal stability of barnase in the presence of urea. *Biochemistry,* **34**, 6795–6804.

Johnson, C. M., Oliveberg, M., Clarke, J. & Fersht, A. R. (1997). Thermodynamics of denaturation of mutants of barnase with disulfide crosslinks. *J. Mol. Biol.* **268**, 198–208.

Katz, B. A. & Kossiakoff, A. (1986). The crystallographically determined structures of atypical strained dis-

ulfides engineered into subtilisin. *J. Biol. Chem.* **33**, 15480–15485.
Kauzmann, W. (1959). Some factors in the interpretation of protein denaturation. *Advan. Protein Chem.* **14**, 1–63.
Kraulis, P. (1991). Molscript, a program to produce both detailed and schematic plots of protein structures. *J. Appl. Crystallog.* **24**, 946–950.
Laity, J. H., Lester, C. C., Shimotakahara, S., Zimmerman, D. E., Montelione, G. T. & Scheraga, H. A. (1997). Structural characterization of an analog of the major rate-determining disulfide folding intermediate of bovine pancreatic ribonuclease A. *Biochemistry,* **36**, 12683–12699.
Lee, B. & Richards, F. M. (1971). The interpretation of protein structures: estimation of static accessibility. *J. Mol. Biol.* **55**, 379–400.
Lee, K. H., Xie, D., Friere, E. & Amzel, L. M. (1994). Estimation of changes in side chain configurational entropy in binding and folding: general methods and applications to helix formation. *Proteins: Struct. Funct. Genet.* **20**, 68–84.
Lees, C. W. & Hartley, R. W. (1966). Studies on *Bacillus subtilis* ribonuclease. III. purification and amino acid composition. *Biochemistry,* **5**, 3951–3960.
Liu, Y. & Sturtevant, J. M. (1996). The observed change in heat capacity accompanying the thermal unfolding of proteins depends on the composition of the solution and on the method employed to change the temperature of unfolding. *Biochemistry,* **35**, 3059–3062.
Makhatadze, G. I. & Privalov, P. L. (1995). Energetics of protein structure. *Advan. Protein Chem.* **47**, 307–425.
Makhatadze, G. I., Clore, G. M. & Gronenborn, A. M. (1995). Solvent isotope effect and protein stability. *Nature Struct. Biol.* **2**, 852–855.
Mayr, L. M., Odefey, C., Schutkowski, M. & Schmid, F. X. (1996). Kinetic analysis of the unfolding and refolding of ribonuclease T_1 by a stopped-flow double-mixing technique. *Biochemistry,* **35**, 5550–5561.
McCrary, B. S., Edmondson, S. P. & Shriver, J. W. (1996). Hyperthermophile protein folding thermodynamics: differential scanning calorimetry and chemical denaturation of Sac7d. *J. Mol. Biol.* **264**, 784–805.
McCrary, B. S., Bedell, J., Edmondson, S. P. & Shriver, J. W. (1998). Linkage of protonation and anion binding to the folding of Sac7d. *J. Mol. Biol.* **276**, 203–224.
McDonald, I. K. & Thornton, J. M. (1994). Satisfying hydrogen bonding potential in proteins. *J. Mol. Biol.* **238**, 777–793.
McNutt, M., Mullins, L. S., Raushel, F. M. & Pace, C. N. (1990). Contribution of histidine residues to the conformational stability of ribonuclease T_1 and mutant Glu-58 → Ala. *Biochemistry,* **29**, 7572–7576.
Mossakowska, D. E., Nyberg, K. & Fersht, A. R. (1989). Kinetic characterization of the recombinant ribonuclease from *Bacillus amyloliquefaciens* (Barnase) and investigation of key residues in catalysis by site-directed mutagenesis. *Biochemistry,* **28**, 3843–3850.
Murphy, K. P. & Friere, E. (1992). Thermodynamics of structural stability and cooperative folding behavior in proteins. *Advan. Protein Chem.* **43**, 313–361.
Myers, J. K. & Pace, C. N. (1996). Hydrogen bonding stabilizes globular proteins. *Biophys. J,* **71**, 2033–2039.
Myers, J. K., Pace, C. N. & Scholtz, J. M. (1995). Denaturant *m* values and heat capacity changes: relation to changes in accessible surface areas of protein unfolding. *Protein Sci.* **4**, 2138–2148.
Myers, J. K., Pace, C. N. & Scholtz, J. M. (1997). Helix propensities are identical in proteins and peptides. *Biochemistry,* **36**, 10923–10929.
Nicholson, E. M. & Scholtz, J. M. (1996). Conformational stability of the *Escherichia coli* HPr protein: test of the linear extrapolation method and a thermodynamic characterization of cold denaturation. *Biochemistry,* **35**, 11369–11378.
Nishimura, S. & Nomura, M. (1959). Ribonuclease of *Bacillus subtilis*. *J. Biochem. (Tokyo),* **46**, 161–167.
Okorokov, A. L., Hartley, R. W. & Panov, K. I. (1994). An improved system for ribonuclease Ba expression. *Protein Express. Purificat.* **5**, 547–552.
Oliveberg, M., Vuilleumier, S. & Fersht, A. R. (1994). Thermodynamic study of the acid denaturation of barnase and its dependence on ionic strength: evidence for residual electrostatic interactions in the acid/thermally denatured state. *Biochemistry,* **33**, 8826–8832.
Pace, C. N. (1986). Determination and analysis of urea and guanidine hydrochloride denaturation curves. *Methods Enzymol.* **131**, 266–280.
Pace, C. N. (1990a). Conformational stability of globular proteins. *Trends Biochem. Sci.* **15**, 14–17.
Pace, C. N. (1990b). Measuring and increasing protein stability. *Trends Biotechnol.* **8**, 93–98.
Pace, C. N. (1995). Evaluating the contribution of hydrogen bonding and hydrophobic bonding to protein folding. *Methods Enzymol.* **259**, 538–554.
Pace, C. N. & Creighton, T. E. (1986). The disulphide folding pathway of ribonuclease T_1. *J. Mol. Biol.* **188**, 477–486.
Pace, C. N. & Grimsley, G. R. (1988). Ribonuclease T_1 is stabilized by cation and anion binding. *Biochemistry,* **27**, 3242–3246.
Pace, C. N. & Laurents, D. V. (1989). A new method for determining the heat capacity change for protein folding. *Biochemistry,* **28**, 2520–2525.
Pace, C. N. & Scholtz, J. M. (1996). Measuring the conformational stability of a protein. In *Protein Structure: A Practical Approach* (Creighton, T. E., ed.), pp. 299–321, IRL Press, Oxford.
Pace, C. N., Grimsley, G. R., Thomson, J. A. & Barnett, B. J. (1988). Conformational stability and activity of ribonuclease T_1 with zero, one, and two intact disulfide bonds. *J. Biol. Chem.* **263**, 11820–11825.
Pace, C. N., Laurents, D. V. & Thomson, J. A. (1990). pH dependence of the urea and guanidine hydrochloride denaturation of ribonuclease A and ribonuclease T_1. *Biochemistry,* **29**, 2564–2572.
Pace, C. N., Heinemann, U., Hahn, U. & Saenger, W. (1991). Ribonuclease T_1: structure, function, and stability. *Angew. Chem. Int. Ed. Engl.* **30**, 343–360.
Pace, C. N., Laurents, D. V. & Erickson, R. E. (1992). Urea denaturation of barnase: pH dependence and characterization of the unfolded state. *Biochemistry,* **31**, 2728–2734.
Pace, C. N., Shirley, B. A., McNutt, M. & Gajiwala, K. (1996). Forces contributing to the conformational stability of proteins. *FASEB J,* **10**, 75–83.
Privalov, P. L. & Gill, S. J. (1988). Stability of protein structure and hydrophobic interaction. *Advan. Protein Chem.* **39**, 193–234.
Privalov, P. L. & Khechinashvili, N. N. (1974). A thermodynamic approach to the problem of stabiliz-

ation of globular protein structure: a calorimetric study. *J. Mol. Biol.* **86**, 665–684.

Privalov, P. L., Tiktopulo, E. I., Venyaminov, S. Y., Griko, Y. V., Makhatadze, G. I. & Khechinashvili, N. N. (1989). Heat capacity and conformation of proteins in the denatured state. *J. Mol. Biol.* **205**, 737–750.

Radzicka, A. & Wolfenden, R. (1988). Comparing the polarities of the amino acids: side-chain distribution coefficients between the vapor phase, cyclohexane, 1-octanol, and neutral aqueous solution. *Biochemistry,* **27**, 1644–1670.

Rico, M., Santoro, J., Gonzalez, C., Bruix, M. & Niera, J. L. (1991). *Structure, Mechanism and Function of Ribonucleases. Proceedings of the 2nd International Meeting Held in Sant Feliu de Guixols, Girona Spain.* (Cuchillo, C. M., de Lorans, R., Nogues, M. V. & Pares, X., eds), pp. 9–14, IBF Publications, Barcelona.

Rosenberg, H. F., Dyer, K. D., Tiffany, H. L. & Gonzalez, M. (1995). Rapid evolution of a unique family of primate ribonuclease genes. *Nature Genet.* **10**, 219–223.

Salahuddin, A. & Tanford, C. (1970). Thermodynamics of the denaturation of ribonuclease by guanidine hydrochloride. *Biochemistry,* **9**, 1342–1347.

Sali, D., Bycroft, M. & Fersht, A. R. (1988). Stabilisation of protein structure by interaction of an alpha-helix dipole with a charged side-chain. *Nature,* **335**, 496–500.

Santoro, M. M. & Bolen, D. W. (1988). Unfolding free energy changes determined by the linear extrapolation method. 1. Unfolding of phenylmethanesulfonyl α-chymotrypsin using different denaturants. *Biochemistry,* **27**, 8063–8068.

Sato, K. & Egami, F. (1957). Studies on ribonucleases in takadiastase. I. *J. Biochem. (Tokyo),* **44**, 753–767.

Schein, C. H. (1997). From housekeeper to microsurgeon: the diagnostic and therapeutic potential of ribonucleases. *Nature Biotech.* **15**, 529–536.

Scholtz, J. M. (1995). Conformational stability of HPr: the histidine-containing phosphocarrier protein from *Bacillus subtilis*. *Protein Sci.* **4**, 35–43.

Schrier, E. E. & Schrier, E. B. (1967). The salting-out behavior of amides and its relation to the denaturation of proteins by salts. *J. Phys. Chem.* **71**, 1851–1860.

Schwarz, F. P. & Kirchoff, W. H. (1988). Biological thermodynamic data for the calibration of differential scanning calorimeters: heat capacity data on the unfolding transition of ribonuclease A in solution. *Thermochimica Acta,* **128**, 267–295.

Sevcik, J., Sanishvili, R. G., Pavlovsky, A. G. & Polyakov, K. M. (1990). Comparison of active sites of some microbial ribonucleases: structural basis for guanylic specificity. *Trends Biochem. Sci.* **15**, 158–162.

Sevcik, J., Dodson, E. J. & Dodson, G. G. (1991). Determination and restrained least-squares refinement of the structures of ribonuclease Sa and its complex with 3′-guanylic acid at 1.8 Å resolution. *Acta. Crystallog. Struct. Sci. sect. B,* **47**, 240–253.

Sevcik, J., Hill, C. P., Dauter, Z. & Wilson, K. S. (1993a). Complex of ribonuclease from *Streptomyces aureofaciens* with 2′-GMP at 1.7 Å resolution. *Acta Crystallog. sect. D,* **49**, 267–271.

Sevcik, J., Zegers, I., Wyns, L., Dauter, Z. & Wilson, K. S. (1993b). Complex of ribonuclease Sa with cyclic nucleotide and proposed model for the reaction intermediate. *Eur. J. Biochem.* **216**, 301–305.

Sevcik, J., Dauter, Z., Lamzin, V. S. & Wilson, K. (1996). Ribonuclease from *Streptomyces aureofaciens* at atomic resolution. *Acta. Crystallog. sect. D,* **52**, 327–344.

Shiao, D. F., Lumry, R. & Fahey, J. (1971). Studies of the chymotrypsinogen family of proteins. XI. Heat-capacity changes accompanying reversible thermal unfolding of proteins. *J. Am. Chem. Soc.* **93**, 2024–2035.

Shirley, B. A., Stanssens, P., Steyaert, J. & Pace, C. N. (1989). Conformational stability and activity of ribonuclease T_1 and mutants: $Gln^{25} \Rightarrow$ Lys, $Glu^{58} \Rightarrow$ Ala, and the double mutant. *J. Biol. Chem.* **264**, 11621–11625.

Shirley, B. A., Stanssens, P., Hahn, U. & Pace, C. N. (1992). Contribution of hydrogen bonding to the conformational stability of ribonuclease T_1. *Biochemistry,* **31**, 725–732.

Spolar, R. S. & Record, M. T. (1994). Coupling of local folding to site-specific binding of proteins to DNA. *Science,* **263**, 777–784.

Spolar, R. S., Livingstone, J. R. & Record, M. T. (1992). Use of liquid hydrocarbon and amide transfer data to estimate contributions to thermodynamic functions of protein folding from the removal of nonpolar and polar surface from water. *Biochemistry,* **31**, 3947–3977.

Steyaert, J. (1997). A decade of protein engineering on ribonuclease T_1: atomic dissection of the enzyme-substrate interactions. *Eur. J. Biochem.* **247**, 1–11.

Swint, L. & Robertson, A. D. (1993). Thermodynamics of unfolding for turkey ovomucoid third domain: thermal and chemical denaturation. *Protein Sci.* **2**, 2037–2049.

Takamine, J. (1914). Enzymes of *Aspergillus oryzae* and the application of its amyloclastic enzyme to the fermentation industry. *Chem. News,* **110**, 215–218.

Tanford, C. (1964). Isothermal unfolding of globular proteins in aqueous urea solutions. *J. Am. Chem. Soc.* **86**, 2050–2059.

Tanford, C. (1970). Protein denaturation, part C. Theoretical models for the mechanism of denaturation. *Adv. Protein Chem,* **24**, 1–95.

Tsong, T. Y., Hearn, R. P., Wrathall, D. P. & Sturtevant, J. M. (1970). A calorimetric study of thermally induced conformational transitions of ribonuclease A and certain of its derivatives. *Biochemistry,* **9**, 2666–2677.

Viguera, A. R., Martinez, J. C., Filimonov, V. V., Mateo, P. L. & Serrano, L. (1994). Thermodynamic and kinetic analysis of the SH3 domain of spectrin shows a two-state folding transition. *Biochemistry,* **33**, 2142–2150.

von Hippel, P. H. & Wong, K. (1965). On the conformational stability of globular proteins. *J. Biol. Chem.* **240**, 3909–3923.

Wintrode, P. L., Makhatadze, G. I. & Privalov, P. L. (1994). Thermodynamics of ubiquitin unfolding. *Proteins: Struct. Funct. Genet.* **18**, 246–253.

Woody, R. W. (1994). Contributions of tryptophan side chains to the far-ultraviolet circular dichroism of proteins. *Eur. Biophys. J.* **23**, 253–262.

Xu, J., Baase, W. A., Baldwin, E. & Matthews, B. (1998). The response of T4 lysozyme to large-to-small substitutions within the core and its relation to the hydrophobic effect. *Protein Sci.* **7**, 158–177.

Yao, M. & Bolen, D. W. (1995). How valid are denaturant-induced unfolding free energy measurements? Level of conformance to common assumptions over an extended range of ribonuclease A stability. *Biochemistry*, **34**, 3771–3781.

Yu, Y., Makhatadze, G. I., Pace, C. N. & Privalov, P. L. (1994). Energetics of ribonuclease T_1 structure. *Biochemistry*, **33**, 3312–3319.

Zhang, T., Bertelsen, E. & Alber, T. (1994). Entropic effects of disulphide bonds on protein stability. *Nature Struct. Biol.* **1**, 434–438.

Edited by P. E. Wright

(Received 30 December 1997; received in revised form 2 March 1998; accepted 3 March 1998)